

Analyst

Accepted Manuscript



This is an *Accepted Manuscript*, which has been through the Royal Society of Chemistry peer review process and has been accepted for publication.

Accepted Manuscripts are published online shortly after acceptance, before technical editing, formatting and proof reading. Using this free service, authors can make their results available to the community, in citable form, before we publish the edited article. We will replace this *Accepted Manuscript* with the edited and formatted *Advance Article* as soon as it is available.

You can find more information about *Accepted Manuscripts* in the [Information for Authors](#).

Please note that technical editing may introduce minor changes to the text and/or graphics, which may alter content. The journal's standard [Terms & Conditions](#) and the [Ethical guidelines](#) still apply. In no event shall the Royal Society of Chemistry be held responsible for any errors or omissions in this *Accepted Manuscript* or any consequences arising from the use of any information it contains.

ARTICLE

Label free sensing of creatinine using a 6 GHz CMOS near-field dielectric immunosensor

Cite this: DOI: 10.1039/x0xx00000x

S. Guha,^{a*} A. Warsinke,^b Ch. M. Tientcheu,^b K. Schmalz,^a Ch. Meliani^a and Ch. Wenger^a

Received 00th January 2012,

Accepted 00th January 2012

DOI: 10.1039/x0xx00000x

www.rsc.org/

In this work we present a CMOS high frequency direct immunosensor operating at 6 GHz (C-band) for label free determination of creatinine. The sensor is fabricated in standard 0.13 μm SiGe:C BiCMOS process. The report also demonstrates the ability to immobilize creatinine molecules on Si_3N_4 passivation layer of the standard BiCMOS/CMOS process, therefore, evading any further need of cumbersome post processing of the fabricated sensor chip. The sensor is based on capacitive detection of the amount of non-creatinine bound antibodies binding to an immobilized creatinine layer on the passivated sensor. The chip bound antibody amount in turn corresponds indirectly to the creatinine concentration used in the incubation phase. The determination of creatinine in the concentration range of 0.88 – 880 μM has been successfully demonstrated in this work. A sensitivity of 35 MHz/10 fold increase in creatinine concentration (during incubation) at the centre frequency of 6 GHz has been manifested by the immunosensor. The results have been compared with a standard optical measurement technique and the dynamic range and sensitivity is of the order of established optical indication technique. The C-band immunosensor chip comprising an area of 0.3 mm^2 reduces the sensing area considerably, therefore, requiring sample volume as low as 2 μl . The small analyte sample volume and label free approach also reduce the experimental costs in addition to the low fabrication costs offered by batch fabrication technique of CMOS/BiCMOS process.

Introduction

Over the last decades, Enzyme Linked Immunosorbent Assays (ELISAs) have been developed as standard methods in clinical diagnostics. In the rapidly growing area of point-of-care testing (POCT), lateral flow assays or as they are frequently referred, immunochromatographic assays, are the commonly used methods¹⁻⁴. However, since the readout gives only qualitative to semi-quantitative results, the application is limited to diagnose diseases which are accompanied with high changes in analyte concentration. In contrast, antibody-based biosensors (immunosensors) are able to measure the analyte quantitatively^{5,6}. However, state of the art immunosensors require several incubation or manual pipetting steps⁷. For easy handling, which is mandatory for POCT, the immunosensor devices should work autonomously. Three different approaches are currently under investigation for such automation. One way is to use an ELISA like immunosensor format for an autonomous working lab-on-a-chip device containing all required reagents (e.g. buffers, enzyme or fluorophor antibody conjugates, and enzyme substrate), separation units, pumps, channels and sensors⁸⁻¹⁰. A second approach also uses labelling compounds (e.g. enzymes, fluorophors, redox mediators) but in

a one-step assay format (mix and measure approach)¹¹. Nevertheless, such labelling techniques often change the properties of antigens and antibodies. Therefore, for each antigen-antibody pair, a new coupling procedure has to be adapted. The third approach involves transduction methods e.g. surface plasmon resonance spectroscopy which allows the direct indication of antigen antibody binding without any labelling compounds¹². However, this technique involves complicated front end circuit integration and complex measurement test-benches. On the other hand, most of the commercially available direct immunosensor devices are highly sophisticated (e.g. BIAcore), requiring well trained personal and are expensive; therefore, making them not suitable for POCT. Electrochemical transduction methods have the potential to circumvent such drawbacks^{9,13-15}. In addition, compatibility of such electrochemical sensors to standard CMOS process technology would further make batch fabrication possible, thereby leading to simpler and cost effective alternative solution to ELISA based approaches. High frequency sensors can be an effective solution to establish such CMOS compatible electrochemical immunosensors.

With the advent of microwave technologies, a fast growing research area of applying high frequency techniques to biological and diagnostic applications has emerged. These high frequency sensors due to their miniaturized size, need very small volumes of probe sample and also require no incubation time, thus making them extremely lucrative for POCT purposes¹⁶⁻¹⁹. Although microwave interaction with bio-molecules, cells, tissues, etc., has been studied for decades²⁰⁻²², such high frequency biosensors have come into existence in the early 2000s. Recently detection of various types of cells has been demonstrated using sensors operating in microwave frequency range. Grenier et al. have shown possible detection of living and dead cells in biological cell suspension using a passive capacitive sensor at frequency range of 1 GHz to 40 GHz²³. Ferrier et al. have also demonstrated characterizing of yeast cells in the frequency range of 1 GHz to 2 GHz, also based on purely passive interferometric structure²⁴. Use of coplanar waveguide arrangement to characterize cells was shown in^{17,25}. CMOS active sensors for labelled sensing techniques using magnetic beads as markers have been further demonstrated by Wang et al²⁶. However, exploring the area of direct immunosensor based on high frequency technique is still on the horizon and is a potential “all-electrical” alternative to the existing immunosensors.

In this report, we describe a novel CMOS direct immunosensor, operating in the C-band of the RF spectrum and has been utilised to identify creatinine concentration. Creatinine is one of the most often determined parameters in clinical diagnostics, since it is an index for renal glomerular filtration rate and function. The concentration range in serum and plasma is about 5-17 $\mu\text{g/mL}$ (44-150 μM). In children or in patients with severe hepatic diseases, advanced liver disease, decreased muscle mass, and general debilitation, creatinine is present in much lower concentrations (3-5 $\mu\text{g/mL}$; 27-44 μM)²⁷. Chemical²⁸ and enzymatic^{29,30} determination methods which are used at present are not very specific or sensitive. Therefore, antibody based creatinine assays and electrochemical immunosensors have been developed by using redox or enzyme labels^{31,32}. In contrast, the proposed approach based on microwave techniques on CMOS platform circumvents the problem of labelling by utilising dielectric properties of creatinine and anti-creatinine antibody molecules³¹ in combination with the aqueous medium used in the experiments.

The sensing principle is based on the variation of capacitance (here an interdigitated capacitor) embedded in a CMOS oscillator, causing a shift in the resonant frequency of the oscillator. The change of capacitance is caused by the variation of fringing electric fields of the interdigitated capacitor (IDC), due to the change of permittivity on top of it. For the proposed dielectric immunosensor the permittivity variation is brought about by the different amounts of anti-creatinine antibodies binding to the creatinine molecules immobilized on the IDC. In this work, for the first time a method to immobilize creatinine molecules on the surface of silicon nitride (Si_3N_4) layers has been demonstrated. Si_3N_4 is the standard passivation layer for CMOS technologies; therefore, the capability of immobilizing creatinine molecules on its surface helps to evade any additional post processing steps for future label free sensors

used in creatinine detection. Thus, a complete CMOS compatible immunosensor is realized with negligible incubation delay and with complete on chip read-out techniques

Materials and Methods

Design and operation of sensor

Multi-fingered planar IDC is used as the prototype capacitive sensor in this work. The sensor IDC along with the complete CMOS oscillator circuit (explained in the subsequent section) is fabricated in the standard 0.13 μm SiGe:C BiCMOS process of IHP technology³³. Fig. 1a shows the BiCMOS back end of line (BEOL) stack with seven metal layers (five thin metal layers and two top thick metal layers). The IDC is fabricated on the penultimate metal layer of thickness 2 μm (referred as TM1) of the BiCMOS stack.

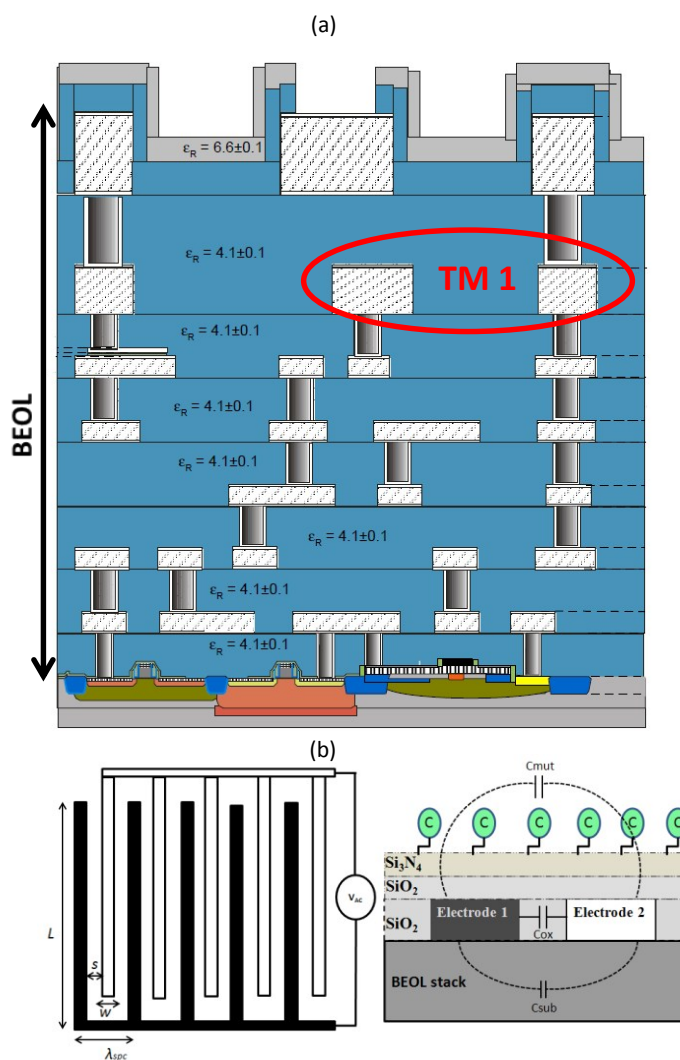


Figure 1: a) Schematic view of 0.13 μm SiGe:C BiCMOS stack with seven metal layers. The IDC is fabricated on the penultimate metal layer marked as TM1 (thickness 2 μm). b) Geometrical parameters of IDC showing the spatial wavelength. The 2D semi-infinite model of a unit cell of the IDC

The IDC geometry and the corresponding 2D semi-infinite model showing the immobilized creatinine molecules are depicted in Fig. 1b. Five fingered IDC with electrode length (L) of 100 μm and equal electrode width (w) and inter-electrode spacing (s) of 20 μm was fabricated. The capacitance of the IDC can be attributed to three major contributing factors: C_{ox} due to the SiO_2 between the electrodes (fingers); C_{sub} due to the fringing electric fields penetrating into the BEOL stack below the TM1 metal layer; C_{mut} due to the fringing electric fields penetrating into the material under test placed on top of the sensor. Often the oxide capacitance is neglected^{34, 35} due to negligible metal layer thickness. However, in this design, the thickness of the IDC electrodes of 2 μm is comparable to the dimension of the electrode spacing and width, thus, C_{ox} is no longer negligible. The total per unit capacitance is given as,

$$C_{IDC} = C_{ox} + C_{mut} + C_{sub} \quad (1)$$

For a given sensor geometry, fabricated in a standard technology, the C_{ox} and C_{sub} contributions in eq (1) are constant. However, for sensor applications, C_{mut} is varied with materials of different permittivity. In this report the varying concentrations of anti-creatinine antibodies binding to the immobilized creatinine layer on the passivated IDC surface cause the permittivity variation. Steps towards the capacitive sensing are depicted in Fig. 2. The creatinine molecules were immobilized on the sensor area of the immunosensor chip initially. The anti-creatinine antibodies were incubated with varied concentrations of creatinine. The resultant solutions were pipetted on top of the sensing area. Following this phase, the chips were washed with water and dried. Further adding the anti-mouse-antibody peroxide conjugate, a binding of this conjugate to the anti-creatinine antibody was observed showing that the anti-creatinine antibody was still bound by chip immobilized creatinine and not released by any denaturation process from the creatinine due to drying phase.

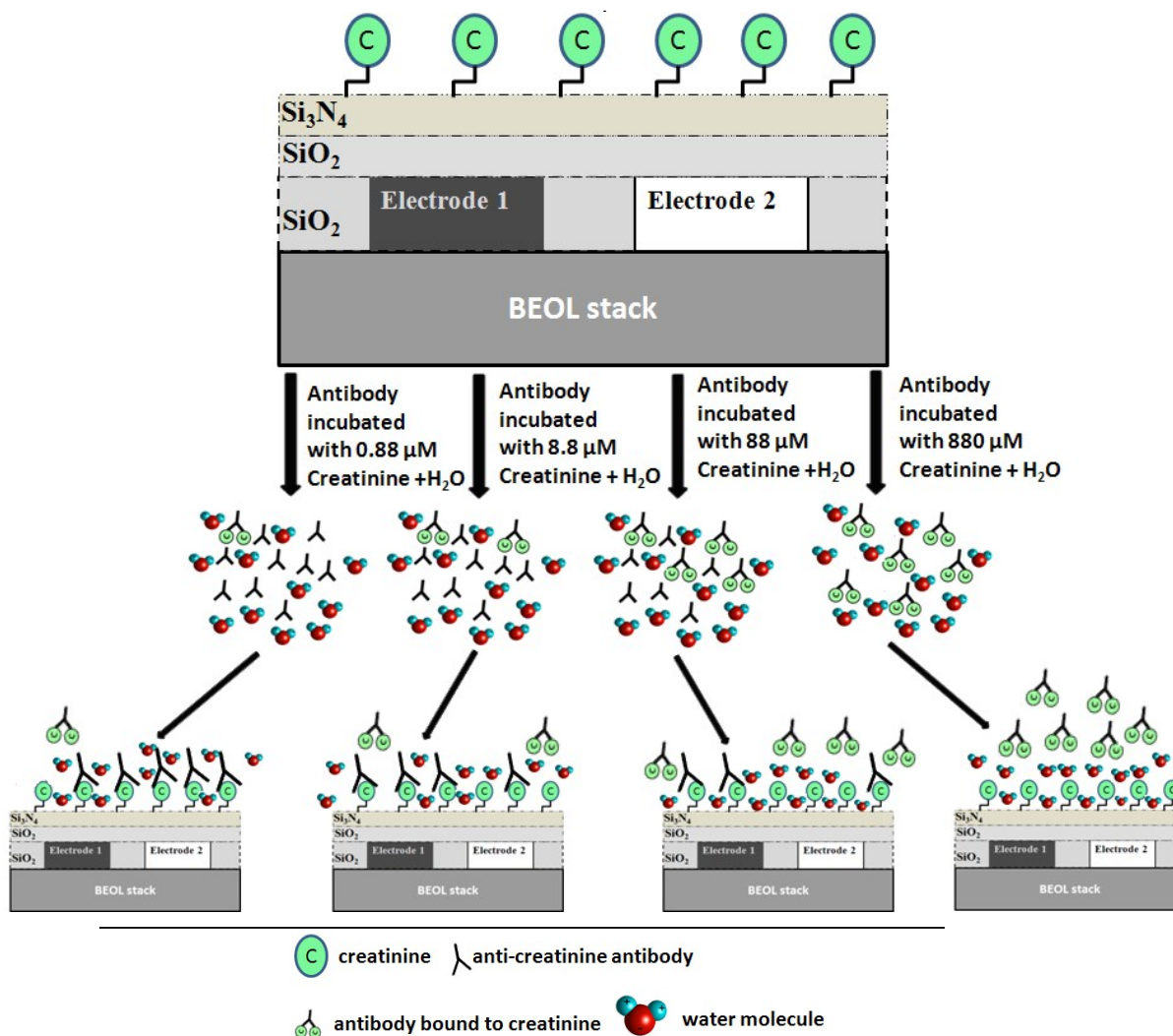


Figure 2: Sensor operation of the dielectric immunosensor. Creatinine molecules had been immobilized on the passivated surface of the sensor. Anti-creatinine antibodies were incubated in four different concentrations of creatinine molecules (pre-treatment phase). The four different antibody solutions are allowed to bind to the immobilized creatinine molecules. Antibody samples incubated with higher concentration of creatinine have less free antibodies left to bind to immobilized creatinine molecules

The additional water molecules shown in the schematic in Fig. 2, depicts the droplet of water that was added during the electrical measurement of the sensor chip. The variation of the amount of non-creatinine bound antibodies (from the incubation step) binding to the immobilized creatinine layer which in turn varies the amount of water molecules surrounding the immobilized layer causes the change of the C_{mut} contribution of the IDC

The use of water in the experiment prompts intrinsic sensitivity amplification, due to considerable permittivity contrast between the antibodies and the water. Anti-creatinine antibodies are incubated with different concentrations of creatinine samples. Four such samples were prepared with creatinine concentration varying from $0.88 \mu\text{M}$ to $880 \mu\text{M}$. Antibodies incubated in lesser concentration of creatinine, bound to more fraction of the immobilized creatinine molecules on the sensor surface in comparison to the ones incubated in higher concentration of creatinine. Higher antibodies binding to immobilized creatinine molecules indicates more number of water molecules being replaced by them from the immobilized creatinine ambient. From sensing perspective, this indicates a capacitive change of the IDC which can be translated to the creatinine concentration used for the incubation step.

Immobilization of creatinine

In order to establish the immobilization surface chemistry for creatinine without any additional post fabrication steps, test chips ($\text{Si}/\text{Si}_3\text{N}_4$) of size 1 cm^2 with Si_3N_4 passivation layer were diced and used to compare different immobilization procedures based on creatinine butyric acid and a creatinine- bovine serum albumin conjugate (crea-BSA). Both compounds were synthesized as described by Benkert et al³¹. Best results regarding antibody binding were obtained by using adsorption of crea-BSA to the Si_3N_4 surface. Therefore, Crea-BSA (10 mg/ml in standard phosphate buffered saline, PBS) was diluted in the ratio 1:10 with aqua bidest. $2 \mu\text{l}$ of this solution was pipetted on the centre of the Si_3N_4 surface of the test chips and incubated in a humid chamber for 1 hour. Control chips were modified with $2 \mu\text{l}$ of a BSA solution in a same way. After six washing steps with PBS and three washing steps with aqua bidest, the chip surfaces were blocked with 2.9 ml 3% BSA in PBS (BSA/PBS) for 1 hour. For detection of immobilized creatinine, 0.1 ml of $3 \mu\text{g}/\text{ml}$ anti-creatinine antibody in BSA/PBS solution was added and incubated for 1 hour. After three washing steps with PBS the chips were incubated for 1 hour with $2, 5 \text{ ml}$ peroxidase-conjugated goat anti-mouse IgG (H+L) which was obtained from Dianova (Germany) and diluted in the ratio 1:5,000 in BSA/PBS. After six washing steps with PBS the chips were incubated with 2.5 ml of a peroxidase standard substrate solution (3,3',5,5'-tetramethylbenzidine, H_2O_2 dissolved in 0.1 M acetate buffer pH 5) for 1 hour and the developed blue colour was compared visually. Since only in the case of chips with crea-BSA an antibody binding was observed it can be concluded that the binding of creatinine- bsa to the chip is

very strong. Moreover, a high concentration of BSA during the incubation with the antibody ensures that no displacement of the crea-BSA by BSA actually takes place.

Sensor circuit design

The multi-fingered sensor IDC is coupled with a pair of inductors to form an LC resonant tank. The oscillation of the resonant tank is driven by a pair of cross-coupled nMOS transistors as shown in Fig. 3. This topology resembles a cross coupled CMOS oscillator³⁶, where the sensor IDC is analogous to the variable capacitor used in such configurations. The cross-coupled transistors add parasitic capacitances in parallel to the sensor IDC. The parasitic capacitance is attributed to the transistors' dimensions³⁶. Wider transistors bring in higher parasitic capacitance. However, the transistors need to be sufficiently wide for optimum gain to sustain the oscillations³⁶. An additional buffer stage is shown, following the core oscillator which is used to isolate the oscillator from the subsequent circuit stages, in order to have an independent sensor operation. In this case, an additional circuitry can be further incorporated to down convert the high frequency output to a DC value for further easier operation and handling capability. The additional transistors in the buffer further add to the parasitic capacitance, thus degrading the overall sensitivity. For a given stable circuit (no variation of circuit operating points), the parasitic capacitive contributions are constant. Therefore, the exclusive variation of the capacitance in the circuit is due to the change in IDC capacitance caused by the varying concentration of anti-creatinine antibodies binding to the creatinine molecules immobilized on the IDC.

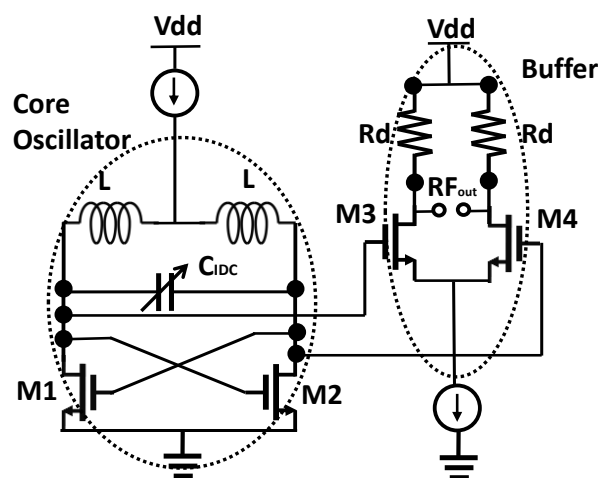


Figure 3: Schematic view of the dielectric sensor circuit. The transistors M1 and M2 drive the oscillations and M3 and M4 constitute the buffer stage. The IDC acts as the variable capacitor for the oscillator

The resonant frequency of the oscillator in the first order approximation is given as

$$f = \frac{1}{2\pi} (2LC)^{-0.5} \quad (2)$$

where, C_{total} is the summation of the capacitance due to the IDC and the parasitic capacitances; L is the inductance of the individual inductors used in the resonant circuit, in this case 1 nH, with a quality factor of 14 at 6 GHz. The capacitance of the IDC in this report is 100 fF. The additional parasitic capacitances due to the cross coupled transistors and the buffer transistors were simulated to be 55 fF. The inductors were fabricated on topmost metal layer of BEOL stack for high quality factor resonator. The sensitivity of such a sensor is defined by the differential change of the resonant frequency with respect to the differential change of the permittivity due to the variation of amount of antibodies binding to the immobilized creatinine molecules.

The “all electrical” measurement requires a standard power supply, supplying up to 3.3 V. Further miniaturization is possible by operating the device with a battery. As mentioned above, the output of the sensor system is an electrical signal around the frequency range of 6 GHz. An X band spectrum analyser from Rohde and Schwarz is used to measure the frequency spectrum.

Results and Discussion

Simulation of capacitance variation

Variation of the capacitance was simulated using FEM tool, COMSOL 4.2a. The immobilized creatinine molecules were modelled as a continuous layer of thickness 10 nm and permittivity of $3 \sim 4^{37,38}$. The antibodies are modelled as cylindrical pillars of height 30 nm and effective diameter 10 nm and a relative permittivity of 2. The antibodies are considerably larger than the creatinine molecules.

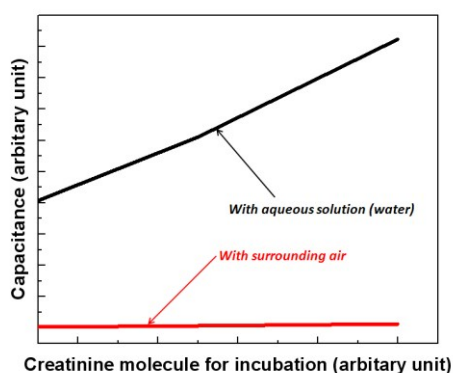


Figure 4: Typical variation of IDC capacitance as a function of concentration of creatinine molecules used in the incubation of antibodies. The capacitance increases with increase in creatinine molecule concentration used during incubation. The capacitance variation is strong when the surrounding medium for experiment is water while with air the variation is negligible

The simulation indicates, for an aqueous solution environment (i.e. when the electrical experiments are performed with an additional drop of water on the sensing area as mentioned above), the capacitance of the IDC increases with the increase in concentration of creatinine molecules used for the incubation of the antibodies (see Fig.4). The result although appears counterintuitive initially, can be explained as a combined effect of the aqueous solution and the antibodies. Higher concentration of creatinine molecules used for incubation indicates lesser number of free antibodies that can bind to the immobilized creatinine layer. With fewer antibodies binding to the immobilized creatinine, a large fraction of creatinine molecules are surrounded by the molecules of aqueous solution. In case of water the permittivity ($\epsilon = 70$ at 6 GHz)²¹ is considerably higher as compared to the antibodies, thus, resulting in a higher capacitance of the IDC. The capacitance variation is strongly dependent on the permittivity contrast between the surrounding medium and the antibodies. Therefore, it is seen with air in the surrounding ($\epsilon=1$), the capacitance is almost constant as the permittivity contrast is very low. Therefore, the use of aqueous solution (water) acts as an intrinsic sensitivity amplifier, magnifying the sensitivity by many folds. From the CMOS oscillator sensor circuit outlook, this change of capacitance translates to a decreasing resonant frequency with increasing concentration of creatinine molecules used for incubation of the antibodies.

Optical measurement of creatinine concentration

Optical measurements were performed with Si_3N_4 test chips to find the best immobilization and test conditions which should be finally applied for the IDC sensor chips. In addition, since the ELISA-like assay procedures and the optical measurements are very reliable³⁹⁻⁴¹, these measurements were also used as independent standard method to compare the results with the electric measurements.

At first, different methods to immobilize creatinine to the Si_3N_4 surface were compared regarding antibody binding. Therefore creatinine butyric acid and crea-BSA were covalently or non-covalently immobilized to different modified test chips. 2 μl of the immobilization solution was pipetted to the Si_3N_4 surface (see Fig.5) which was the same amount which was needed to cover the IDC sensor area, marked red in Fig. 8.

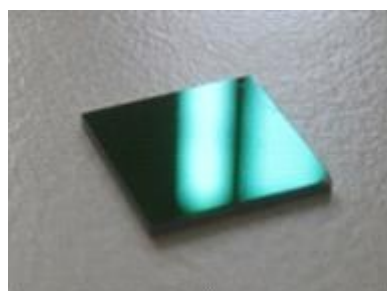


Figure 5: Chip photograph of $\text{Si}_3\text{N}_4/\text{Si}$ test chip for optical measurement

The immobilized creatinine was then detected with the monoclonal anti-creatinine antibody B90-AH5 and a peroxidase-conjugated anti-mouse IgG. The peroxidase activity was detected via a standard colour reaction using TMB and hydrogen peroxide. Most of the chips generated no colour. Only chips with adsorptive immobilized crea-BSA generated the typical blue colour whereas chips with immobilized BSA generated no colour. This result shows that the monoclonal anti-creatinine antibody was specifically bound to the immobilized crea-BSA. For creatinine determination an indirect competitive immunoassay principle shown in Fig. 6 was applied. Therefore, the crea-BSA modified Si_3N_4 test chips were incubated with different creatinine concentrations (0 - 8.8 mM) with a defined and beforehand optimized antibody concentration (0.1 $\mu\text{g}/\text{ml}$). Creatinine competes thereby with the chip-immobilized creatinine for the creatinine binding sites of the antibody. As higher the creatinine concentration as fewer antibodies can bind to chip-immobilized creatinine.

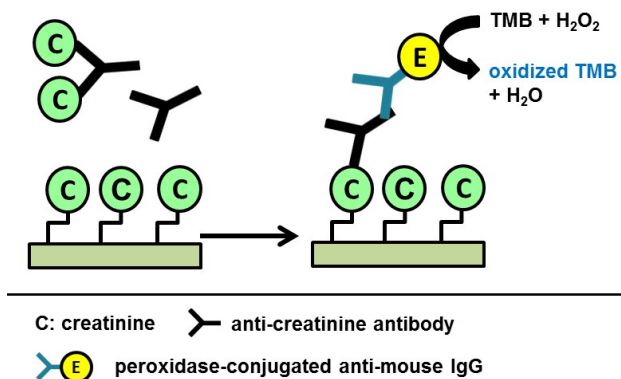


Figure 6: Indirect competitive assay principle for optical creatinine determination with creatinine-modified Si_3N_4 test chips

The resultant concentration dependency for creatinine is shown in Fig. 7, with the dynamic range of measurement ranging from 0.88- 88 μM . This covers perfectly the clinically relevant range if taken into account that the antibody and buffer have to be added to the serum or plasma sample.

As mentioned above, the optical measurements were conducted to compare the standard technique with our proposed “all-electrical” approach. The dynamic range of the established optical technique although covers the concentration range of creatinine which is of clinical relevance, but is saturated beyond 88 μM of creatinine concentration. On comparing the dynamic range of both measurement techniques, the electrical approach shows an order of magnitude increase in dynamic range, as is demonstrated in the subsequent section.

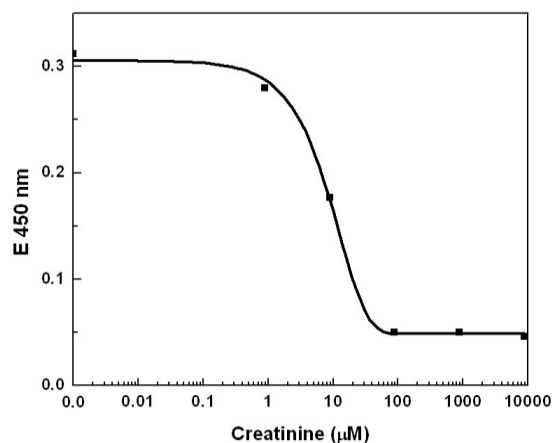


Figure 7: Optical measurement of creatinine concentration. The response slope of the optical measurement in the range 0.88 to 88 μM shows the dynamic range of the standard measurement technique

Dielectric measurement of creatinine concentration

Characterisation of sensor

The chip photograph depicting the IDC sensor along with the oscillator circuit is shown in Fig. 8. Electrical characterization of the chips was performed before calibration and creatinine measurements. The chip draws a current of 27 mA from a 3.3 V DC supply. The resonant frequency of the oscillator was 6.01 GHz in air (with no material on top of the sensor). The chip has an area of 0.3 mm^2 . The performance of the sensor oscillator showing resonant frequency shift for varying IDC capacitance was characterized with glucose solution varying measurements.

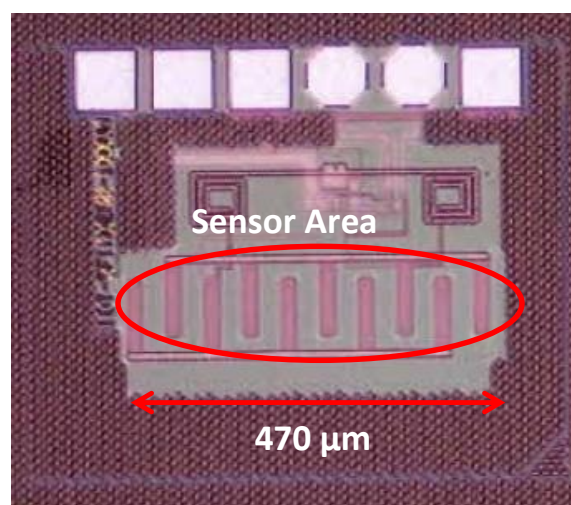


Figure 8: Chip photograph of dielectric sensor. The sensor area (IDC) is marked in red

Different concentrations of glucose solution were pipetted on the sensing area and the resulting frequency was measured and compared with simulations, as shown in Fig. 9. It is observed that the resonant frequency up-shifts for increasing concentration of glucose in a solution. The behaviour can be attributed to the decrease in resultant permittivity of the solution with increasing concentration of glucose; glucose has a lower permittivity as compared to water. With lower glucose concentration the resultant solution has permittivity close to the permittivity of water, thereby yielding the resonant frequency of the oscillator close to the one with water on top of IDC.

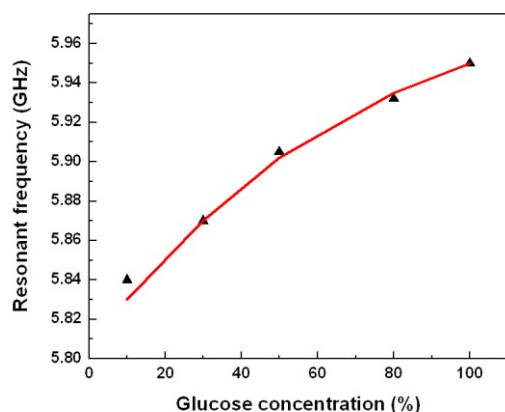


Figure 9: Calibration of sensor circuit with glucose solution. The red curve shows the simulation and the black triangles are the measurement results. The resonant frequency up-shifts with increasing glucose concentration

This measured behaviour of the sensor is in close agreement with the theoretical and simulated behaviour of the sensor. Thus the working of the sensor was well established with the calibration technique and further extension to a direct immunosensor was undertaken.

Creatinine concentration measurement

In order to characterize the reproducibility of the sensor chip from the process technology aspect, it is necessary to characterize (study the frequency response) several chips from the same wafer. Multiple chips on the same wafer were characterized to estimate the on wafer process variation. The resonant frequency of the oscillator varied not more than 3 MHz. This depicts the high yield and reproducibility of the sensor chip. Eight such chips with same resonant frequency of 6.01 GHz were treated later for immobilization of creatinine molecules on the sensor layers. 2 μ l of the pre-treated anti-creatinine antibody samples were pipetted on the Si₃N₄ based surface of the IDC sensor area (marked in red in Fig.8). As mentioned in the previous section, a drop of water (1 μ l) was added on the sensor area during electrical measurement in order to have a strong permittivity contrast and a better sensor response. Fig. 10 shows the resonant frequency shift of two chips treated with two different incubated antibody samples. The output power level of -20 dBm is much

higher than the noise level but also optimum, in order to not damage the creatinine molecules and also antibodies binding to it.

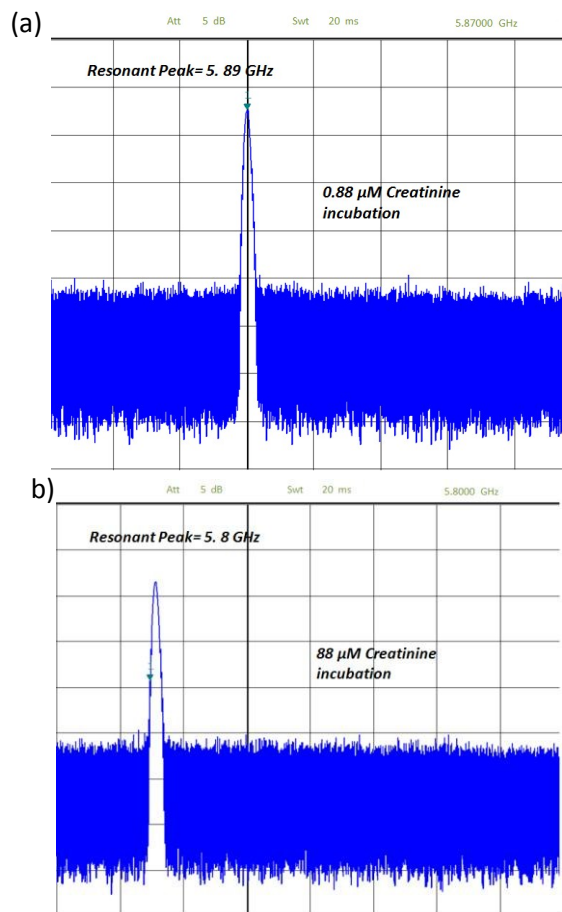


Figure 10: a) Resonant frequency peak for chip treated with antibodies incubated with 0.88 μ M creatinine. b) Resonant frequency peak for chip treated with antibodies incubated with 88 μ M creatinine

The measurement results of the chips with four different samples of antibody are shown in Fig. 11. The higher the concentration of creatinine in the pre-incubation the lower is the concentration of antibody binding to the immobilized creatinine molecules on the IDC. The black curve shows the measurements done with an additional droplet of water of approximate volume of 1 μ l carefully pipetted on the sensing area. This was explained in the previous section. It is seen with lower concentration of creatinine used in pre-treatment (higher amount of antibodies binding to the immobilized creatinine), higher is the resonant frequency. This is accredited to the fact that a higher concentration of antibodies binding to the creatinine molecules, replace more amount of water molecules previously surrounding the creatinine molecules. The antibodies having a much lower permittivity compared to water, reduces the effective permittivity as sensed by the IDC. Therefore, there is a frequency downshift for decreasing antibody concentration or increasing creatinine concentration in the incubation phase. As seen from the measurements, for each step variation of the

concentration of the creatinine, the resonant frequency varies by approximately 35 MHz. With highest creatinine concentration during the incubation phase, least amount of antibodies binds to the immobilized creatinine molecules on the IDC. Therefore, the resulting resonant frequency tends towards the frequency of the oscillator with pure water on top of it (5.73 GHz). The red curve shows the same experiments done on the same chips with air as the surrounding medium.

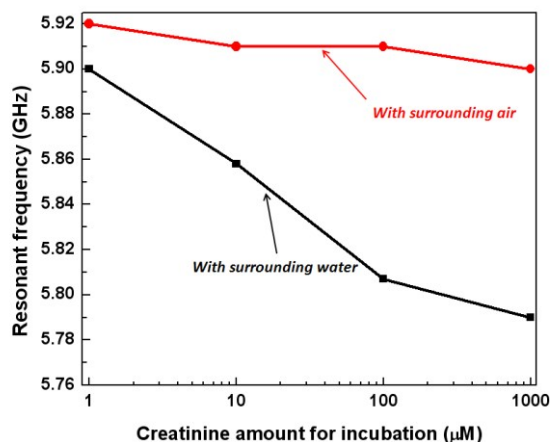


Figure 11: Measured variation of resonant frequency as a function of creatinine concentration used in the incubation of antibodies. The black curve shows the resonant frequency for four samples with increasing concentration of creatinine used in incubation while the experiment was done in aqueous (water) environment. The resonant frequency downshifts with increasing creatinine concentration. The red curve shows the same experiment done with air as the surrounding medium

As seen from the results there is negligible variation of the resonant frequency of the oscillator although there is a tendency of frequency downshift. The measurement results agree closely with our proposed model and simulation. The capacitance variation of the IDC is strongly dependent on the permittivity contrast between the antibodies and the surrounding medium and hence, suited for biosensor, immunosensor applications as most often a buffer solution is used for such measurements.

It can also be noted from the above measurements that in aqueous solution, the sensor has a dynamic range higher than the optical measurement technique. It was shown in Fig.7 that the measurement response with optical technique saturates beyond 88 µM of creatinine concentration used in the incubation phase. However, in the proposed sensor, the curve although seems to have a saturating effect, but have considerable sensitivity from 88 µM to 880 µM. The variation of frequency in this range is 25 MHz and is considerably higher than the process variation of 3 MHz, therefore, showing an order of magnitude higher dynamic range compared to the established optical technique. This can be attributed to the contrast of permittivity between water molecules and the anti-

creatinine antibodies. When comparing the sensitivity of the two approaches, the percentage change of frequency per 10 fold increase in concentration of creatinine with respect to the total frequency shift over the entire dynamic range (~42%) is comparable to the percentage change in E_{450nm} intensity (~40%).

Error bar measurement

In order to determine the error bar in the measurement and also to determine the reproducibility of the sensor system from the measurement perspective, several sets of chips with same samples of pre-incubated antibodies were measured at the same time in aqueous solution. The maximum standard deviation in the resonant frequency for similar measurement condition is 0.223. The frequency response of two sets of chips showing maximum measurement variations were plotted. The resonant frequency contrast for the two sets of chips was observed for all the four antibody samples incubated with different amounts of creatinine. The maximum drift in the resonant frequency of two chips with same sample of antibodies was observed to be 4 MHz, shown in Fig.12. This drift in the resonant frequency is approximately a tenth of the measured sensitivity of the sensor. The observed variation being considerably less than the sensitivity shows high reproducibility of the immunosensor system.

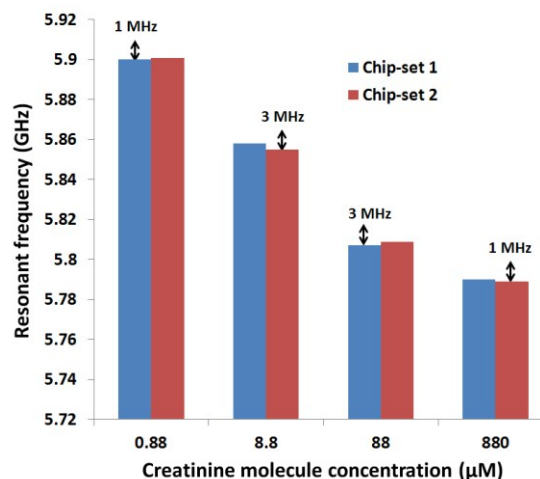


Figure 12: Error bar measurement for two sets of chips. The maximum frequency drift does between two chips does not exceed 4 MHz

Conclusions

The results show that creatinine can be measured with the developed CMOS high frequency dielectric immunosensor in the clinically relevant concentration range. The electrical measurement results show close agreement with an optical standard measurement techniques. The measurement capability in the order of nanomolar concentration level shows that such a high frequency sensor can be successfully used for relevant

measurements in clinical diagnostics. The measured frequency shift of 35 MHz in the clinically relevant regime of creatinine concentration of 0.88 μM to 88 μM is much higher than the effect of process variation. The effect of process variation was measured and was shown negligible in comparison to the sensitivity of the sensor. This was shown in the error bar measurement conducted with two sets of chips. Therefore, it can be deduced that the demonstrated CMOS high frequency sensor has considerable stability for clinical measurements. The miniaturized sensor design and the exclusion of any labelling compounds will reduce the costs in comparison to other antibody-based creatinine assays enormously. Additionally the capability of immobilization of creatinine molecules on standard passivation layer of CMOS process (Si_3N_4) evades the need of any post processing techniques of the silicon chip required for immobilization of creatinine molecules. This result is very significant for future CMOS immunosensors for creatinine and can be adapted to other antigen antibody couples. Since the already published creatinine enzyme immunoassays and indirect immunosensors can specifically measure creatinine in real human serum samples it can be assumed that the developed immunosensor which uses the same antibody is also able to measure real samples. Since nanomolar analyte concentrations can be determined it can be stated that in future the developed technology can be adapted for other clinically relevant analytes as well.

Acknowledgements

This work was supported by the grant from the federal state of Brandenburg and the European Regional Development Fund. The authors would also like to thank the Technology department of IHP for chip fabrication

Notes and References

- a. IHP, Im Technologie Park 25, 15236, Frankfurt (Oder), Germany
 - b. University of Potsdam, Institute of Biochemistry and Biology, Karl-Liebknecht-Str. 24-25, 14476 Potsdam, Germany
- *contact author (guha@ihp-microelectronics.com)

1. A. Warsinke, *Anal Bioanal Chem.*, 2009, **5**, 1393-405
2. S. Feng, R. Caire, B. Cortazar, M. Turan, A. Wong and A. Oczan, *ACS Nano*, 2014, **8** (3), 3069-3079
3. P. Sithigorngul, S. Rukpratanporn, N. Pecharaburanin, P. Suksawat, S. Longyant, P. Chaivisuthangkura and W. A. Sithigorngul, *J. microbial. Methods*. 2007, **71**, 256-264
4. T. Peng, W. Yang, W. Lai, Y. Xiong, H. Wei and J. Zhang, *Anal Methods* 2014, **6** 7394-7398
5. A. P. F. Turner, *Nature Biotechnol.* 1997, **15**, 421
6. M. Mohammed and M. P. Desmulliez. *Lab Chip*, 2011, **11**, 569-595
7. Y. Wan, Y. Su, X. Zhu, G. Liu, and C. Fan, *Biosensors Bioelectronmics*, 2013, **47**, 1-11

8. F. F. Bier and S. Schumacher, *Adv Biochem Eng Biotechnol.*, 2013, **133**, 1-14
9. F. Ricci, G. Adornetto and G. Palleschi, *Electrochimica Acta*, 2012, **84**, 74-83
10. J. Li, Q. Xu, X. Wei and Z. Hao. *J. Agric. Food Chem.*, 2013, **61**(7), 1435-1440
11. A. Warsinke, *Adv Biochem Engin/Biotechnol.*, 2008, **109**, 155-193
12. G. Gauglitz *Analytical and Bioanalytical Chemistry*, 2010, **398**, 2363-2372
13. F. Ricci, G. Volpe, L. Micheli and G. Palleschi, *Analytica Chimica Acta* 2007, **605**, 111
14. Q. Zhu, R. Yuan, Y. Chai, J. Han, Y. Li and N. Liao. *Analyst*, 2013, **138**, 620-626
15. V. Mani, B. Chikkaveeraiah, V. Patel, J. S. Gutkind and J. F. Rusling. *ACS Nano*, 2009, **3**(3), 585-594
16. S. Guha, F.I. Jamal, K. Schmalz, Ch. Wenger and C. Meliani. Conf. Proc. IEEE MTT-S International Microwave Symposium 2014
17. Y. Chen, H. Wu, Y. Hong and H. Lee B. *Biosensors and Bioelectronics* 2014, **61**, 417-421
18. L. Li and D. Uttamchandani. *IEEE Sensors Journal*. 2009 **9**(12), 1825-1830
19. K. Grenier and D. Dubuc, Conf. Proc. IEEE MTT-S International Microwave Symposium 2015
20. R. Pethig and D.B. Kell, *Phys. Med. Biol.*, 1987, **32**, 933-970
21. C. Gabriel, S. Gabriel, and E. Corthout, *Phys.Med.Biol*, 1996, **41**, 2231-2249
22. T. Hanai, N. Koizumi, and A. Irimajiri, *Biophys. Struct. Mechanism*, 1975, **1**, 285-294
23. K. Grenier, D. Dubuc, T. Chen, F. Artis, T. Chretiennot, M. Poupot, and J. Fournie, *IEEE-TMTT*, 2013, **61**, 2023-2030
24. G. A. Ferrier, S. F. Romanuik, D. J. Thomson, G. E. Bridges and M. R. Freeman, *Lab on a Chip*, 2009, **9**, 3406-3412
25. Y. Yang, H. Zhang, J. Zhu, G. Wang, T. R. Tzeng, X. Xuan, K. Huang, and P. Wang, *Lab on a chip*, 2010, **10**, 553-555
26. H. Wang, C. Sideris, A. Hajimiri, Conf. Proc. *Custom Integrated Circuit Conference*, 2010, 1-4
27. D. Johnson, *Clinical Chemistry* (Ed. E. H. Taylor), 1989, 55-82
28. M.Z. Jaffe, *Physiol. Chem.* 1896, **10**, 391
29. P. Fossati, *Clin. Chem.* 1983, **29**, 1494
30. A. W. Wahlefeld, G. Herz, H. U. Bergmeyer, *Scand.J. Clin. Lab. Invest. Suppl.* 1972, **29**,
31. A. Benkert, F. Scheller, W. Schoessler, C. Hentschel, B. Micheel, O. Behrsing, G. Scharte, W. Stoecklein, and A. Warsinke, *Anal Chem*, 2000, **72**, 916-92
32. A. Benkert, F. W. Scheller, W. Schoessler, B. Micheel, A. Warsinke, *Electroanalysis*, 2000, **12**, 1318-1321
33. H. Riicker, et al, *IEEE Electronic Devices Meeting (IEDM)*, 2007, 651-654
34. R. Igrreja and C. J. Dias, *Sensors and Actuators A*, 2004, **112**, 291-301
35. L. A. Ramajo, D. E. Ramajo, M. M. Rebored, D. H. Santiago and M. S. Castro, *Materials research*, 2008, **11**, 471-476

- 1
2
3
4
5
6
7
8
9
10
11
12
13
14
15
16
17
18
19
20
21
22
23
24
25
26
27
28
29
30
31
32
33
34
35
36
37
38
39
40
41
42
43
44
45
46
47
48
49
50
51
52
53
54
55
56
57
58
59
60
36. T.H. Lee, The design of CMOS Radio Frequency Integrated Circuits, Cambridge
37. P. Kukic, D. Farrell, L. P. MacIntosh, B. Garcia-Moreno E, K. S. Jensen, Z. Toleikis, K. Teilum and J. E. Nielsen, *J. Am. Chem. Soc.* 2013, **135** (45), 16968-16976
38. L. Li, C. Li, Z. Zhang and E. Alexov, *J. Chem.Theory Comput.* 2013, **9**, 2126-2136
39. S. Nicolardu, S. Herrera, M. J. M. Bueno and A. R. Fernandez-Alba. *Anal. Methods* 2012, **4**, 3364-3371
40. S. Sun, M. Yang, Y. Kostov and A. Rasooly. *Lab Chip* 2010, **10**, 2093-2100
41. T. G. Henares, Y. Uenoyama, Y. Nogawa, K. Ikegami, D. Citterio, K. Suzuki, S. Funano, K. Sueyoshi, T. Endo and H. Hisamoto. *Analyst* 2013, **138**, 3139-3141